# C$_\alpha$−C Backbone Fragmentation Dominates in Electron Detachment Dissociation of Gas-Phase Polypeptide Polyanions

**Frank Kjeldsen,\*[a, b] Oleg A. Silivra,[a] Igor A. Ivonin,[a] Kim F. Haselmann,[b] Mikhail Gorshkov,[c] and Roman A. Zubarev[a]**

**Abstract:** Fragmentation of peptide polyanions by electron detachment dissociation (EDD) has been induced by electron irradiation of deprotonated polypeptides $[M-nH]^{n-}$ with $>10$ eV electrons. EDD has been found to lead preferentially to $a^\bullet$ and $x$ fragment ions (C$_\alpha$−C backbone cleavage) arising from the dissociation of oxidized radical anions $[M-nH]^{(n-1)-\bullet}$. We demonstrate that C$_\alpha$−C cleavages, which are otherwise rarely observed in tandem mass spectrometry, can account for most of the backbone fragmentation, with even-electron $x$ fragments dominating over radical $a^\bullet$ ions. Ab initio calculations at the B3LYP level of theory with the 6-311+G(2p,2d)//6-31+G(d,p) basis set suggested a unidirectional mechanism for EDD (cleavage always N-terminal to the radical site), with $a^\bullet,x$ formation being favored over

$a,x^\bullet$ fragmentation by 74.2 kJ mol$^{-1}$. Thus, backbone C$_\alpha$−C bonds N-terminal to proline residues should be immune to EDD, in agreement with the observations. EDD may find application in mass spectrometry for such tasks as peptide sequencing and localization of labile post-translational modifications, for example, those introduced by sulfation and phosphorylation. EDD can now be performed not only in Fourier transform mass spectrometry, but also in far more widely used quadrupole (Paul) ion traps.

## Introduction

In proteomic studies, tandem mass spectrometry (MS/MS) has recently become a key methodology,[1] with electrospray ionization (ESI) being one of the two preferred ionization techniques.[2] MS/MS involves the dissociation of gas-phase polypeptide ions, often of tryptic peptides from either isolated proteins or protein mixtures. MS/MS provides primary sequence information for library-based protein identification and the determination of post-translational modifications (PTMs).[3]

[a] F. Kjeldsen, O. A. Silivra, I. A. Ivonin, Prof. R. A. Zubarev
BioMedical Center, Laboratory for Biological and Medical Mass Spectrometry
Box 583, Uppsala University, 75123 Uppsala (Sweden)
Fax: (+46)18-471-7209
E-mail: frank.kjeldsen@bmms.uu.se

[b] F. Kjeldsen, Prof. K. F. Haselmann
Department of Chemistry
University of Southern Denmark
5230 Odense M (Denmark)

[c] Prof. M. Gorshkov
The Institute of Energy Problems of Chemical Physics
Moscow (Russia)

For the purpose of ion dissociation, different activation techniques have been employed. The most commonly used is collision-activated dissociation (CAD),[4] in which a heterolytic, charge-induced peptide (C−N) bond cleavage in protonated molecular species leads to $b$ and $y'$ fragment ions (see the peptide fragmentation nomenclature in the relevant literature[5,6]). In many respects, collision activation is analogous to thermal heating. In both processes, labile groups, including many types of PTMs, are lost prior to backbone cleavage, which hinders their assignment. This drawback is overcome in electron capture dissociation (ECD),[7] in which specific S−S and N−C$_\alpha$ backbone bond cleavages occur more readily than PTM losses[8,9] and noncovalent complex dissociation.[10] Furthermore, ECD at electron energies ranging from 3 to 13 eV (so-called hot electron capture dissociation, HECD)[6] allows distinction of isomeric isoleucine and leucine residues, which enables complete or nearly complete de novo sequencing of proteins as large as 15 kDa.[11,12]

However, ECD is only applicable to multiply charged positive ions, while many naturally occurring peptides are acidic (~50%) and thus more readily produce negative ions. The groups attached by such common PTMs as phosphorylation,[13] sulfation,[14] sialic acid containing glycosylation,[15] and even acetylation[16] of basic amines (e.g., in lysine side

chains) make polypeptide molecules even more acidic. Although a number of recent publications in the scientific literature have shown that useful sequence information can be derived from CAD mass spectra of negative polypeptide ions,[17,18] negative-ion fragmentation is still rarely used in practice. This is because the spectra obtained from negative-ion MS/MS experiments are rife with ion peaks resulting from internal fragmentations, extensive side-chain losses, and neutral losses from fragments, and therefore these spectra are not always easy to interpret.[19]

Some time ago, our group proposed a novel ion-electron fragmentation technique for polyanions termed electron detachment dissociation (EDD).[20,21] The advantage of ion-electron reactions is that the fragmenting species are odd-electron ions, in which the presence of a radical site diminishes the strength of nearby bonds. If the radical site is located on the backbone, ion-electron reactions lead to extensive backbone fragmentation with labile PTMs being preserved on the fragments.[8,10,22,23] The mechanisms of many ion-electron reactions nevertheless remain obscure. Recently, as we expanded mechanistic studies to EDD, we detected a new prominent feature of this reaction, namely the dominance among backbone cleavages of $C_\alpha-C$ bond ruptures yielding $a^\bullet$ and $x$ ions. This type of cleavage is otherwise rarely observed: $C_\alpha-C$ backbone cleavages have only been reported as being dominant upon photodissociation (PD) of singly-charged cations with UV light of wavelength 157 nm.[24,25] Here, we present experimental and theoretical evidence that, in contrast to 157 nm UV PD of even-electron species, the $C_\alpha-C$ cleavage in EDD involves a radical mechanism with oxidized $[M-nH]^{(n-1)-\bullet}$ ions as reactive intermediates.

## Results

To start with experimental evidence, consider the EDD spectrum of the peptide FAP (Ac-EDLIEDLILE) shown in Figure 1. The general features of the spectrum bear resemblance to the EDD spectra of other peptides.[20,21] The spectrum is dominated by the oxidized (charge-reduced) species and small losses from them (vide infra). Backbone cleavages are also very abundant: overall, all but two inter-residue bonds (78%) have evidently been cleaved, with three $a^\bullet$, one $b$, and five $x$ ions being observed. In comparison, CAD of the $[M-H]^-$ ions gave rise to two $b$, one $y'$, and one $z$ backbone fragment ion (data not shown). $C_\alpha-C$ fragmentation accounted for 96% of all the various EDD backbone cleavages, with $x$ ions dominating over $a^\bullet$ ions by 50%. The most abundant $x$ ions, $x_8^-$ and $x_9^-$, were due to cleavages adjacent to aspartic acid (DL bond) and glutamic acid (ED bond), respectively. The least abundant $x$ ion, $x_7^-$, arose from bond cleavage between the hydrophobic LI pair, while the most abundant $a^\bullet$ ion ($a_5^\bullet$) was due to ED bond cleavage.

The observed preference for backbone fragmentation to occur in the vicinity of acidic residues can be rationalized as follows. FAP is an acidic peptide (pI < 3.6), containing five acidic amino acid residues. Among these are the glutamic
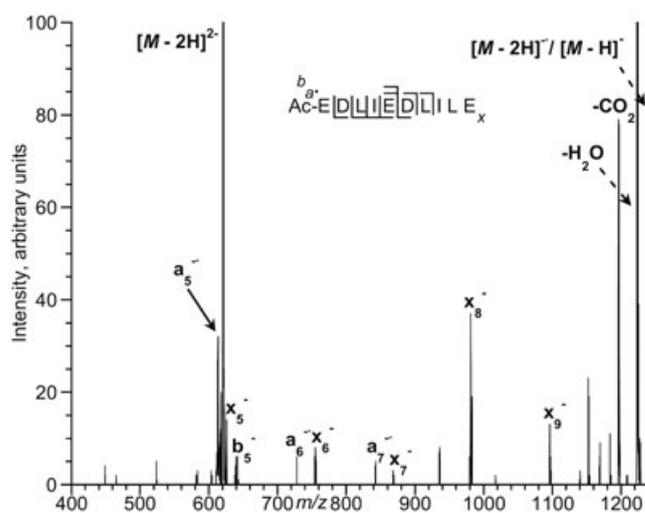


Figure 1. QIT EDD mass spectrum of 2− ions of the FAP peptide (Ac-EDLIEDLILE). $a^\bullet,x$ ions accounted for 96% of the total backbone cleavage abundance.

acid and aspartic acid residues, which, together with the C-terminal carboxylic acid, comprise the most likely candidates for deprotonation. The negative charge of deprotonated groups can be delocalized over other functionalities, for example backbone amides, through what is effectively solvation, such functionalities acting as a protic solvent. It has been suggested[20] that EDD cleavage occurs near the location (or solvation) of the negative charge. Since functional groups in close proximity to the deprotonation site are more likely to participate in charge solvation than more distant groups, EDD backbone cleavage should occur near acidic residues. On the other hand, since hydrophobic side chains (effectively equivalent to an aprotic solvent) do not provide for charge stabilization, which reduces the probability of charge solvation near hydrophobic residues, EDD cleavage in their vicinity should be disfavored, which is also in agreement with the observations.

Examination of the region of the EDD spectrum corresponding to oxidized species reveals that it contains a mixture of $[M-2H]^{-\bullet}$ and $[M-H]^-$ molecular ions. The latter species are frequently observed in EDD and may originate from either proton-transfer reactions between dianions and radical cations formed by electron ionization during the EDD event, or from H$^\bullet$ atom transfer from unidentified neutral species to the oxidized radical anions.[20] The even-electron species $[M-H]^-$ are likely to be responsible for the observed prominent water loss.[18] A radical-initiated mechanism of $CO_2$ loss from oxidized species, another prominent EDD feature, has been suggested elsewhere.[20] In comparison, CAD of the $[M-H]^-$ ions led to abundant neutral losses ($H_2O$ and $NH_3$) from both fragments and precursor ions, but no loss of $CO_2$. In the mass region $m/z$ 1140–1200 of the EDD spectrum, a number of losses from the oxidized species of as yet unidentified origin were found.

The dominance of $a^\bullet$ and $x$ type fragment ions in EDD of the peptide FAP was puzzling, since only $a$ ions have been

reported as dominating for EDD of 2– anions of the sulfated peptide caerulein (pEQDY(SO$_3$H)TGWMDF).[20] The cited study was performed with a Fourier transform ion cyclotron resonance (FTICR) mass spectrometer, while a quadrupolar ion trap (QIT) was employed in the present study. To assess the influence of the instrumental factor, we performed EDD on the 2– anion of caerulein in our QIT set-up, and obtained three *a*· and two *x* ions (Scheme 1),

$$\overset{a\cdot}{pE} \; Q \;|\; D \; \overset{*}{Y} \;|\; T \;|\; G \; W \; M \;|\; D \;|\; F \underset{x}{} - NH_2$$

Scheme 1.

arising from a total of five out of nine possible inter-residue cleavages. No other types of backbone fragment were detected, in contrast to the FTICR results. Oxidized species were more abundant with QIT than with FTICR. Note that one *x* ion in the QIT spectrum originated from bond cleavage adjacent to aspartic acid. The abundance of *a*· ions was 75 % higher than that of the *x* ions.

Other features of the EDD spectra, such as extensive small losses, were similar for both instruments. Importantly, fragment ions obtained in the QIT set-up retained the sulfate group so that the site of sulfation could be unambiguously assigned to Tyr$_4$. To ensure that the observed preference for C$_\alpha$–C bond breakage was not related to a particular peptide sequence, vibrational excitation (CAD) of caerulein dianions was performed. As in FTICR MS, this led to neutral losses, including losses of water and SO$_3$, but little in the way of C–N backbone cleavage (*b* and *y* ions).

The caerulein results may be explained by the much higher background pressure in the QIT instrument ($10^{-3}$ Torr) compared to the FTICR instrument ($10^{-9}$ Torr). Because of the low number of collisions under the ultrahigh vacuum FTICR conditions, the internal energy increment obtained in an ion-electron interaction cannot be rapidly dissipated, which makes backbone fragmentation channels other than C$_\alpha$–C bond rupture possible, although *b* and *y* type fragment ions originating from vibrational excitation of even-electron precursors are not usually observed. The high rate of collisions with background gas in QIT, on the contrary, allows for rapid dissipation of the excess internal energy, promoting only the most energetically favorable fragmentation channels. The higher abundance of intact oxidized species in QIT relative to the overall distribution of fragments is consistent with this collisional stabilization (vide supra).

The time scale of the EDD cleavage is an important issue that is related to the analytical potential of the phenomenon. EDD is a more energetic phenomenon than ECD, because of the difference in the electron energies involved (>10 eV vs. <1 eV). However, if the backbone fragmentation in EDD is fast and/or specific, labile post-translational modifications may remain on the fragments, which would permit PTM mapping. Both the FTICR and QIT results with caerulein are indicative of such a possibility. However,

phosphorylation is a more frequently used and arguably more important modification than sulfation. Therefore, the phosphopeptide VNTEpYPTDLISGV-NH$_2$ was used to test the PTM retention in EDD. The EDD spectrum obtained in the QIT is shown in Figure 2. Three *a*· and three *x* fragments



Figure 2. QIT EDD mass spectrum of 2– ions of the phosphopeptide (VNTEpYPTDLISGV-NH$_2$). Three *a*· and three *x* ions unambiguously determine the site of phosphorylation at the Tyr$_5$ residue.

were observed (the *x* ions dominated by 66 %), all of which retained the phosphate group. Cleavages of a total of six backbone bonds narrowed the phosphorylation site to the EYP sequence, thus excluding the threonine (Thr$_3$ and Thr$_7$) and serine (Ser$_{11}$) residues as potential phosphorylation sites and unambiguously assigning it to the tyrosine residue (Tyr$_5$). In comparison, the CAD spectrum of the 2– anions exhibited consecutive losses of water and phosphate (−79 Da) (data not shown). Thus, EDD can be used for the determination of phosphorylated sites even in peptides that exhibit severe phosphate losses by CAD.

Although electrospray ionization in the negative-ion mode is best suited to acidic peptides, basic peptides also produce abundant polyanion signals. A key question, however, is whether the presence of acidic functionalities is essential for C$_\alpha$–C fragmentation in EDD. To address this issue, we analyzed substance P (RPKPQQFFGLM-NH$_2$), which is very basic (theoretical pI = 11.5) and lacks carboxylic acid functionalities. Despite the high basicity of substance P, negative-ion mode ESI yielded almost as high a current of dianions as that of dications at positive polarity. EDD of dianions of substance P led to extensive fragmentation in the QIT (Figure 3a), with the spectrum featuring four *a*· and five *x* ions, as well as two *y*′ and one *z* fragment. Overall, eight backbone cleavages had evidently occurred. The majority of backbone cleavages were due to C$_\alpha$–C dissociation, with *x* ions accounting for 81 % of the backbone fragment ion signal.

The high yield of dianions was consistent with the earlier observation that, although acidic peptides are not easily ion-

Figure 3. a) QIT EDD mass spectrum of 2− anions of substance P amidated at the C-terminus. Five *x*, two *y′*, one *z*, and four *a•* fragment ions arise from cleavages of eight peptide bonds. b) QIT EDD mass spectrum of 2− anions of substance P (carboxylic acid at the C-terminus) displaying five *x*, one *z*, and three *a•* ions. c) FTICR EDD mass spectrum of 2− anions of the acidic form of substance P giving five *x* and four *y′* ions.

ized in the positive-ion mode, almost all peptides, regardless of their acidity, can be ionized in the negative-ion mode with satisfactory ion abundances.[26] After the hydrogens of the carboxylic groups located at the C-terminus and on the side chains, the next most acidic hydrogens are those positioned on the amide nitrogen atoms. We performed ab initio (B3LYP/6-311+G(2d,2p)//6-31+G(d,p)) calculations on $N$,2-dimethylpropanamide, which showed the hydrogen on the backbone nitrogen to be more acidic than that at the α-carbon atom by 70.8 kJ mol$^{-1}$ (Scheme 2).
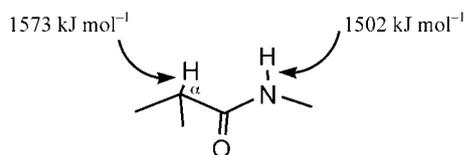


Scheme 2.

This result is in agreement with recent data by Bowie et al., who, at a lower level of theory (HF/6-31G(d)//6-31G(d)), found the amide hydrogen to be more strongly acidic in energetic terms than that at the α-carbon atom by 116 kJ mol$^{-1}$.[27]

Thus, in substance P, deprotonation would be expected to occur at the backbone amide nitrogens. Not surprisingly, the otherwise ubiquitous $CO_2$ loss was absent in EDD of this molecule. Instead, $NH_3$ loss and a low abundance isocyanic acid (CONH) loss were observed.

To investigate the effect of the negative charge localization on the EDD fragmentation pattern, EDD of the acidic form of substance P (with a deamidated C-terminal) was performed (Figure 3b). A series of $x$ ions dominated the spectrum, with $x_7$ being the most abundant, similar to the situation seen in the spectrum of the amidated form (Figure 3a). The $x_9$ ion, however, was suppressed, and extensive $CO_2$ loss was observed (with ~30% of the abundance of $[M-2H]^{-\bullet}$). This loss was a consequence of deprotonation of the C-terminal carboxylic acid, which, upon oxidation by irradiation with energetic electrons, is known to undergo facile decarboxylation.[20,21] This abundant $CO_2$ loss (−44 Da) can be compared with a minor (0.5% of $[M-2H]^{-\bullet}$) isocyanic acid (CONH) loss (−43 Da) from the C-terminus of the amidated form (Figure 3a).

To assess the dependence of the EDD fragmentation pattern on the instrumental conditions, the same samples were analyzed by FTICR MS. The high-resolution FTICR data confirmed the identity of $a^{\bullet}$[20] and $x$ ions as odd- and even-electron species, respectively. As an example, the FTICR EDD mass spectrum of the acidic form of substance P is shown in Figure 3c, obtained by irradiation of the $[M-2H]^{2-}$ ions with 15 eV electrons for 250 ms. Here, $x$ ions again dominate among the backbone fragments, in agreement with preferential charge retention by the C-terminal carboxylic acid. The overall correlation between the relative abundances of $x$ ions normalized with respect to the oxidized species $[M-2H]^{-\bullet}$ found in both spectra was very high, $r > 0.99$ (Figure 3c), which highlights their similarity.

However, $a^{\bullet}$ ions were absent in the FTICR mass spectrum, while two $a^{\bullet}$ fragment ions (one with a low abundance) were detected in the QIT spectrum. This fact is consistent with the earlier observation that less stable EDD products are more abundant in QIT spectra, which was attributed to the 10$^6$-fold higher pressure inside the QIT instrument compared to the FTICR instrument. Apparently, the stabilising effect of pressure outweighs the destabilising effect of the higher effective temperature of ions stored in the QIT. In FTICR, the low frequency of ion–neutral collisions leads to much longer relaxation times after activation through inelastic collisions with electrons, which results in a higher average temperature of ions during the time interval after the EDD event and before detection. Consequently, the $y'$ ions that usually result from thermal (vibrational) excitation are more frequent and abundant in FTICR MS than in QIT. Despite this difference, the notable overall similarity between FTICR and QIT mass spectra indicates that the EDD fragmentation patterns are less determined by the instrumental conditions than by other factors, presumably the locations of the deprotonation and charge solvation sites.

## Discussion

Summarizing the above observations, a consistent feature of EDD is the dominance of $C_\alpha$–C backbone cleavages yielding radical $a^{\bullet}$ and even-electron $x$ ions. This dominance is apparent in terms of both fragment occurrence and ion abundances. Whenever carboxylic groups are present, they give rise to abundant losses of $CO_2$ from the oxidized species.

These $C_\alpha$–C cleavages are rarely produced by most activation techniques. Reilly et al. suggested that absorption of a 157 nm photon by a backbone carbonyl group would lead to homolytic $C_\alpha$–C bond rupture yielding $a^{\bullet}$ and $x^{\bullet}$, with the latter subsequently losing H$^{\bullet}$ atoms.[24] In EDD with $>10$ eV electrons, specific excitation of a certain group is unlikely, and the oxidized radical species $[M-2H]^{-\bullet}$ are the most probable precursors for $C_\alpha$–C cleavages. To test this hypothesis and to attempt to rationalise other experimental results, ab initio calculations were performed on a model system consisting of a complex between the dipeptide H-Gly-Ala-OH and deprotonated acetic acid, the latter representing the C-terminus or the side chain of either Asp or Glu (Figure 4). Calculated total and relative energies of all optimized structures are listed in Table 1.

In the absence of a solvent, that is in vacuo, energy minimization typically occurs through intramolecular charge solvation (charge–dipole interactions).[28] Therefore, as a starting point, the deprotonated carboxylate group **1** was allowed to approach the dipeptide **2**. Local energy minima were obtained for the dipeptide in both the *cis*-amide and *trans*-amide isomeric structures. The *trans*-amide configuration of **2** turned out to be 41 kJ mol$^{-1}$ more stable. Two stable configurations were detected for the *trans*-amide structure, the first with the N-terminal amine group forming hydrogen
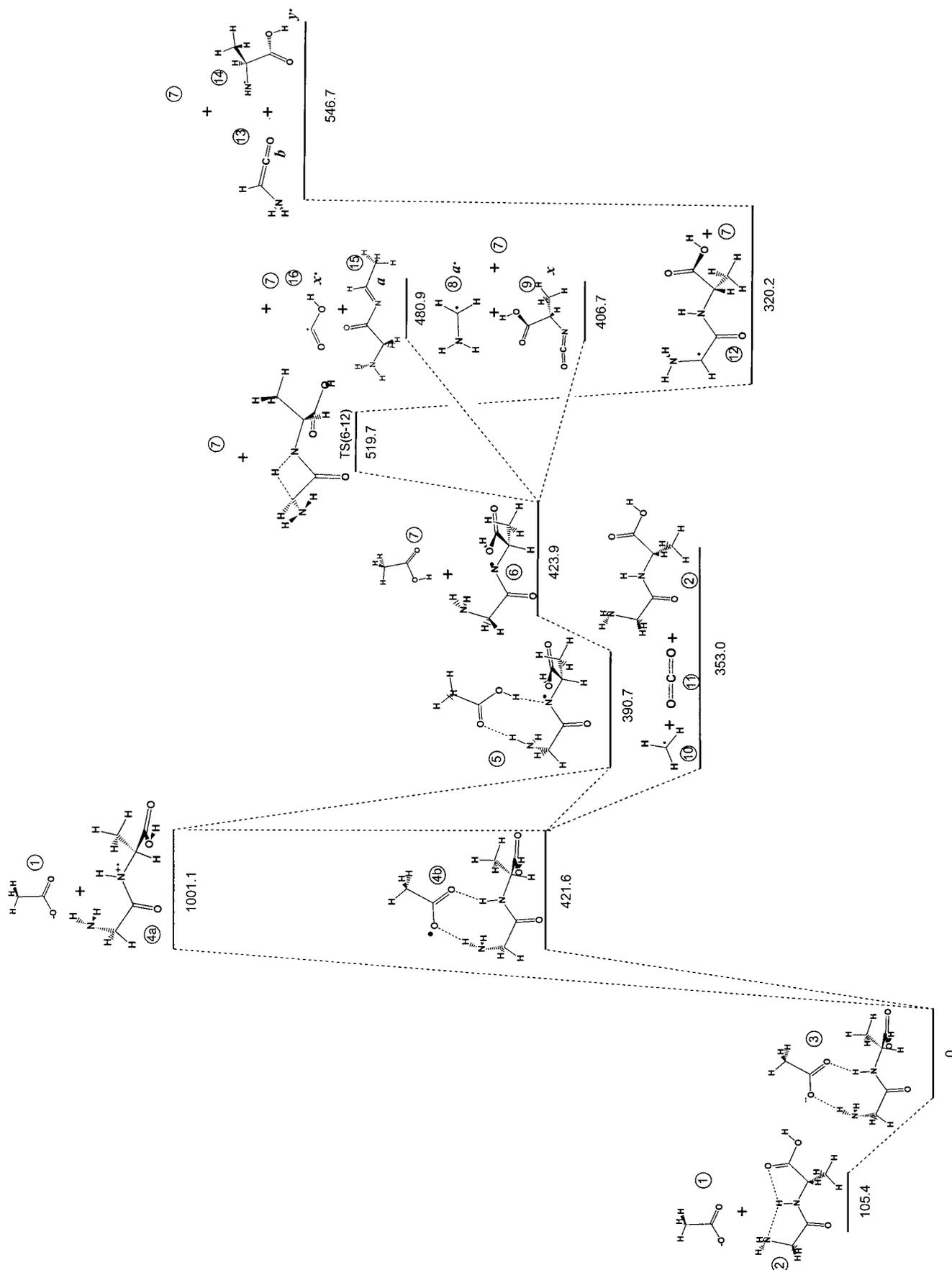
Figure 4. Energy profile of species involved in the EDD mechanism as calculated at the B3LYP/6-311+G(2d,2p)//6-31+G(d,p) level of theory.

Table 1. Total energies (Hartree) and relative energies (kJ mol$^{-1}$).

| Compound | Total electronic energies, $E_t$ [Hartree] | Scaled ZPE correction at 0 K [Hartree] | ZPE corrected energies, $E_{ZPVE}$ [Hartree] | Relative energies $\Delta E_{ZPVE}$ [kJ mol$^{-1}$] |
|---|---|---|---|---|
| **1** | −228.608275 | 0.046065 | −228.562209 | |
| **2** | −531.949589 | 0.157356 | −531.792233 | |
| **1+2** | | | 760.354442 | 105.4 |
| **3** | −760.599989 | 0.205397 | −760.394592 | 0 |
| **4a** | −531.606244 | 0.155140 | −531.451103 | |
| **4a+1** | | | −760.013312 | 1001.1 |
| **4b** | −760.436279 | 0.202258 | −760.234021 | 421.6 |
| **5** | −760.449587 | 0.203818 | −760.245769 | 390.7 |
| **6** | −531.263732 | 0.143405 | −531.120327 | |
| **TS(6–12)** | −531.222267 | 0.138451 | −531.083815 | |
| **7** | −229.172097 | 0.059274 | −229.112823 | |
| **6+7** | | | −760.233150 | 423.9 |
| **TS(6–12)+7** | | | −760.196639 | 519.7 |
| **8** | −95.241648 | 0.048194 | −95.193454 | |
| **9** | −436.024099 | 0.090674 | −435.933425 | |
| **7+8+9** | | | −760.239702 | 406.7 |
| **10** | −39.857414 | 0.028644 | −39.828770 | |
| **11** | −188.650244 | 0.011117 | −188.639127 | |
| **2+10+11** | | | −760.260130 | 353.0 |
| **12** | −531.304235 | 0.144405 | −531.159830 | |
| **12+7** | | | −760.272653 | 320.2 |
| **13** | −208.015204 | 0.048170 | −207.967034 | |
| **14** | −323.196276 | 0.089769 | −323.106507 | |
| **7+13+14** | | | −760.186364 | 546.7 |
| **15** | −342.070404 | 0.118619 | −341.951785 | |
| **16** | −189.166918 | 0.020100 | −189.146818 | |
| **7+15+16** | | | −760.211426 | 480.9 |

bonds to the carbonyl oxygen (not shown), and the second with hydrogen bonding between the same amine nitrogen and the amide hydrogen. The latter configuration **2** was found to be more favorable by about 5 kJ mol$^{-1}$.

Upon charge solvation, strong hydrogen bonding is created between the carboxylate and the amide hydrogen in **3** (1.774 Å). This is consistent with the known polarization of the carbonyl oxygen (partial negative) and the amide hydrogen (partial positive), which maximizes their potential to solvate polar groups and charges. In EDD, an energetic electron induces vertical ionization in **3** and forms either **4a+1** by removing an electron from the free lone-pair on the backbone amide nitrogen, or oxidises the carboxylate group to yield **4b**. The energy required is lower for **4b** (421.6 kJ mol$^{-1}$, ≈4 eV) than for **4a+1** (1001.1 kJ mol$^{-1}$, ≈10 eV). The larger potential energy stored in **4a+1** allows it to proceed exothermically through all suggested channels of fragmentation. Thus, **4a+1** can yield either **4b** by a 580 kJ mol$^{-1}$ exothermic recombination of the positive charge on the backbone with the negative charge on the carboxylate, or **5** by a 610 kJ mol$^{-1}$ exothermic proton transfer from the amide nitrogen to the carboxylate. The carboxyl radical complex **4b** is the most probable intermediate of the decarboxylation leading to loss of CO$_2$ (**11**) and leaving the radical at the side chain of the acidic residue (**10**). This dissociation is exothermic by 69 kJ mol$^{-1}$. If the CO$_2$ loss occurs from the C-terminal carboxyl radical, it will result in an $a_n^\bullet$ ion, $n$ being the number of residues in the peptide. An

alternative pathway for **4b** is to undergo hydrogen abstraction leaving a radical site at the amide nitrogen (**5**), which is exothermic by 31 kJ mol$^{-1}$. The higher exothermicity of decarboxylation is the likely reason for the experimentally observed abundant CO$_2$ loss.

Separation of the carboxy group from the backbone **5** → **6** + **7** is endothermic by 33 kJ mol$^{-1}$. Overall, the subsequent dissociation into $a^\bullet$ (**8**) and $x$ (**9**) fragment ions is exothermic by 15 kJ mol$^{-1}$ with respect to **4b** and exothermic by 594 kJ mol$^{-1}$ with respect to **4a+1**.

A 1,3-hydrogen shift in complex **6** leading to **12** is of relatively high exothermicity (104 kJ mol$^{-1}$), but has to overcome a barrier of 96 kJ mol$^{-1}$ **TS(6–12)**, for which there may be energetic or kinetic obstacles. If formed, **12** may dissociate through endothermic C−N bond cleavage to $b$ (**13**) and $y^\bullet$ (**14**), which would be endothermic by 227 kJ mol$^{-1}$.

The computational data on the EDD mechanism are in general agreement with the experimentally obtained results. The calculations suggest that the lowest-energy channel of backbone fragmentation is the formation of $a^\bullet$ and $x$ ions, which competes with decarboxylation. The formation of other products, for example, $b$ and $y^\bullet$ ions, is disfavored. This is consistent with the observation of a low number of backbone fragments originating from cleavages other than C$_\alpha$−C. Some of these fragments may even be formed from even-electron precursor dianions by way of a thermal mechanism, such as collisional heating during isolation in the QIT.

**Influence of the C-terminal group on EDD fragmentation**: ECD of dications of substance P in both its acidic and amide forms leads to similar mass spectra, with differences being localized at the C-terminus.[29] Differences in the EDD spectra of dianions of the same molecules were more pronounced. This is illustrated in Figure 5, for which the correlation factor for $x$ ion abundances was calculated to be 0.58. The main difference between the two EDD mass spectra was due to the $x_7$ and $x_9$ ions, which can be rationalized in terms of the different sites of deprotonation and charge solvation in the two molecules. Deprotonation will be favored at the carboxylic acid as compared to the amide group (typical gas-phase acidities for carboxylic acids ~1400–1430 kJ mol$^{-1}$; for primary amides ~1470–1500 kJ mol$^{-1}$).[30] Hence, the positions of the negative charges should be *shifted* towards the N-terminus in the amidated form, as opposed to the acidic form, in which it is certainly the C-terminus that is deprotonated. Since the C$_\alpha$−C EDD cleavages are postulated to occur at or near the sites of negative charge solvation, the charge shift towards the N-terminus can account for the fact that $x_9$ ions arising from cleavage near the N-terminus are more abundant in the amidated form. Thus, it appears that the differences in ion abundances in EDD spectra can reflect the secondary gas-phase structure of peptide polyanions, in much the same way as ECD is used to probe the secondary structure of polycations.[31] This suggestion needs to be further tested in a more systematic investigation.
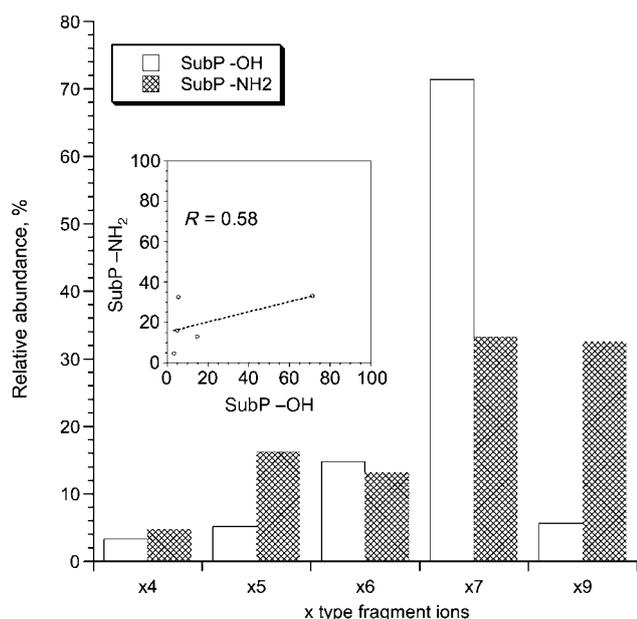
Figure 5. Correlation of EDD product ion abundances of x ions from substance P in acidic and amidated forms.

**Low abundance of radical $a^{\bullet}$ ions**: The almost universally observed lower abundance of radical $a^{\bullet}$ fragment ions compared to the even-electron $x$ ions is believed to be a result of two factors. The first is the lower stability of radicals compared to even-electron species. Thus, radical $a^{\bullet}$ ions may rapidly rearrange and/or undergo secondary decomposition in the gas phase. For instance, in ECD and especially in HECD, radical $z^{\bullet}$ fragment ions usually appear with a lower frequency and intensity than the complementary even-electron $c'$ ions. The $a^{\bullet}$ radical ions may be even less stable than $z^{\bullet}$ fragments. Ab initio calculations have shown that it requires 12–22 kJ mol$^{-1}$ more energy to induce partial side-chain loss in Ile and Leu residues for $z^{\bullet}$ precursors as compared to $a^{\bullet}$ ions.[6] Such a secondary fragmentation of $a^{\bullet}$ ions should lead to even-electron $d$ fragments, which, however, remain to be detected in EDD spectra, most probably due to the low abundances of the precursor $a^{\bullet}$ ions. The question of $d$ ion formation in EDD is of analytical importance, because these species allow the isomeric Ile and Leu residues to be distinguished, which, in turn, is valuable in de novo sequencing of polypeptides.[11] Another expected outcome of the fragmentation of $a^{\bullet}$ ions is the loss of a side chain from the adjacent amino acid residue leading to $e$ ions (N-terminal equivalent of C-terminal $u$ ions formed via a γ-lactam ring, as found in HECD of polycations).[12] The detection of these $d$ and $e$ ions in EDD will be a goal of future studies.

The second contributing factor to the dominance of $x$ ions is the deprotonation of the C-terminus, a common feature of acidic forms of peptides. The energy threshold for detachment of an electron is equal to the electron affinity of the corresponding radical site minus the coulombic repulsion with other negative charges. This threshold depends upon the acidity, as more acidic sites tend to have higher electron

affinities. Thus, if the C-terminus is the most acidic site in the molecule, the electron will be preferentially detached from the other deprotonated site in the dianion, while the C-terminus will remain a mere spectator, preserving its charge to yield C-terminal product ions. As an example, calculations at the B3LYP/6-311+G(2d,2p)//6-31+G(d,p) level have shown that it takes only about 259.8 kJ mol$^{-1}$ to remove an electron from the conjugate base of $N$-methylacetamide (CH$_3$CON$^-$CH$_3$), whereas it takes 421.6 kJ mol$^{-1}$ in the case of acetate (CH$_3$COO$^-$) (Figure 4).

**Directionally restricted mechanism (unidirectional fragmentation)**: The question of the direction in which the α-cleavage proceeds in EDD is important for rationalizing the observed EDD fragmentation pattern. Experimental evidence suggests that the EDD mechanism preferentially leads to cleavage N-terminal to the radical site. An indication of this is the absence of $a^{\bullet},x$ ions originating from cleavage of the $C_\alpha$–C bond N-terminal to the proline residue. For instance, EDD of substance P in both acidic and amide forms produces a series of abundant $x$ ions ranging from $x_4$ to $x_9$. However, the $x$ ions that would have arisen from cleavages N-terminal to Pro, $x_8$ and $x_{10}$, are absent in this series (Figure 3a–c).

The absence of such cleavages is easily rationalized in terms of the unidirectional EDD mechanism, in which the radical site is located on the amide nitrogen. Since proline residues contain a tertiary amide, the abstraction of a hydrogen atom or a proton is impossible. Hydrogen bonding to this nitrogen by other heteroatoms is equally impossible, and the proline residue does not participate in solvation of the negative charge. However, cleavage N-terminal to proline would still occur if the radical site at the adjacent N-terminal amide could initiate $C_\alpha$–C bond rupture in the C-terminal direction. The absence of these cleavages is a strong argument in favor of $C_\alpha$–C bond rupture propagation towards the N-terminus from the radical site.

Another important piece of evidence supporting this conclusion is the dominance among $a$ ions found in EDD of radical $a^{\bullet}$ ions, with all $x$ ions being even-electron species. This $a^{\bullet},x$ formation can only occur if the radical initiates the attack towards the N-terminal side, since the alternative C-terminal directed α-cleavage should produce $a$ and $x^{\bullet}$ ions (Scheme 3).
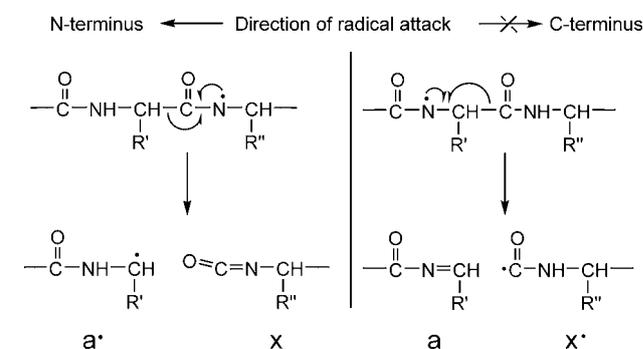


Scheme 3.

Furthermore, ab initio calculations have shown that formation of $a^{\cdot},x$ fragments (**8**, **9**) is more favorable than that of $a,x^{\cdot}$ products (**15**, **16**) by 74 kJ mol$^{-1}$, lending additional support to the unidirectional fragmentation mechanism.

## Conclusion

Fragmentation reactions between negative ions of polypeptides and free electrons observed in a QIT are reported for the first time to lead to dominant $C_{\alpha}{-}C$ fragmentation resulting in $a^{\cdot}$ and $x$ fragment ions. $C_{\alpha}{-}C$ dissociation dominates for both acidic and basic peptides, as well as for peptides with PTMs. The most abundant species in EDD are C-terminal species, and in this respect EDD of polyanions is complementary to ECD of polycations, which favors N-terminal $c'$ ions. The suggested unidirectional mechanism of EDD, supported by high level calculations, explains the formation of $a^{\cdot}$ and $x$ fragments and the immunity to EDD of $C_{\alpha}{-}C$ bonds N-terminal to proline residues. The fact that selected backbone bonds, either $N{-}C_{\alpha}$ or $C_{\alpha}{-}C$ bonds, can be specifically cleaved by appropriate choice of ion-electron reaction underlines the wonderful diversity of the chemistry of peptide radicals. Further studies in this area are clearly necessary.

Analytically, EDD has the potential for polypeptide sequencing and for mapping labile PTMs. The utility of EDD is reinforced by the broader applicability[26] of the negative ESI mode for peptides as compared to the positive mode. However, in order for EDD to become a useful complement to CAD and ECD of positive ions, the fragmentation efficiency needs to be improved. At present, the EDD fragmentation efficiency is of the order of 2–15% in QIT and 5–20% in FTICR mass spectrometry.

Extension of EDD to routine LC/MS/MS analysis of peptide mixtures, which is traditionally performed only in positive-ion mode, should improve the sequence coverage of proteins in these experiments, thus advancing the combined top-down, bottom-up approach for rapid and sensitive PTM mapping in proteins.[23] Since it is believed that PTM analysis will become one of the most important issues in proteomic research,[32] such an advance will be welcome news for the furtherance of this field.

## Experimental Section

**Mass spectrometry**: A modified Esquire LC (Bruker Daltonik AG, Bremen, Germany) QIT mass spectrometer was used in the experiments (Figure 6). The modification included the installation of an electron source based on a heated filament. The filament consisted of one or two parallel "tungsten/rhenium alloy" wires, each 75 µm thick, installed instead of the second lens (lens 2) in front of the first (source-side) end-cap. At all times, except during the irradiation event, the heating current through the filament was kept low and it was biased positively (3–5 V) to prevent electrons from entering the ion trap. During the electron irradiation event, the potential on the center of the filament was kept close to ground, while the current through the wires was raised sufficiently to cause them to glow with a bright-red color. The electron current pro-
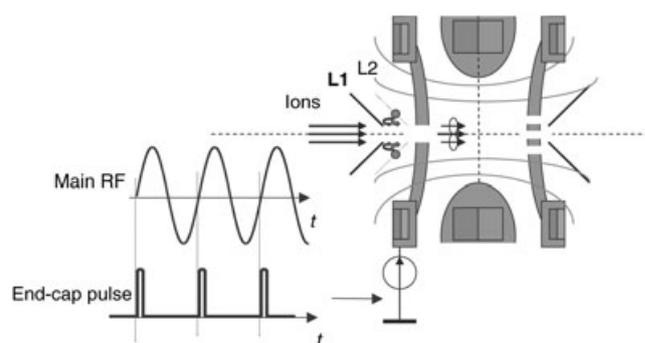


Figure 6. Schematic representation of the modified quadrupolar ion trap (QIT), including the installation of an electron source and permanent magnets on both the ring and the end caps. Injection of electrons was initiated by pulsing of the front end cap once every fundamental rf period during the irradiation event.

duced by the filament was measured at the exit end-cap in the steady-flow regime and reached a few µA.

To maximize the interaction time of ions and electrons, trapping of the injected electrons in the QIT was accompanied by the creation of a static magnetic field together with the existing electrical field. This resulted in the trapping of electrons within the quadrupole trap for up to a half-period (~600 ns)[33] of the rf oscillations. The magnetic field was created by permanent magnets arranged about the ring electrode and on each end-cap electrode. A 5.02 mm groove was cut 12.20 mm into the ring electrode and an aluminium frame with inset magnets was inserted in the groove. The measured magnetic field in the center of the trap was 250 gauss.

Two pulse generators were used to control the energy and duration of the electron irradiation. The electron injection was initiated by positively biasing ($+10$ V) the front end cap for 20–50 ns once every rf period. An electron energy between 10 and 20 eV was selected for optimal results, which was achieved by injecting the electrons in the phase of the rf voltage when the potential in the center of the trap was $+10$ to $+20$ V. The relationship between rf phase and electron energy was established by monitoring the abundances of the $SF_6^{-\cdot}$ and $SF_5^{+}$ ions formed from $SF_6$ gas.

The peptides to be analyzed were electrosprayed in negative-ion mode by means of direct infusion. Ions were accumulated inside the trap for 200–400 ms before isolation of the precursor ion. The pulsed electron irradiation lasted between 200 and 400 ms, with an electron pulse in each fundamental period having a duration of 20–50 ns. Spectra built up from 1 to 500 individual scans were integrated in each experiment. Noise spikes and low-abundance ion peaks that possessed no isotope pattern were filtered out by applying a specially designed automatic routine.

**Sample preparation**: Peptide molecules were purchased from Sigma or synthesized in-house by means of a solid-phase $N$-$\alpha$-Fmoc strategy[34] using a ResPep automatic peptide synthesiser (Intavis AG, Germany). Polypeptides were dissolved in $H_2O$/MeOH (50:50, v/v) to a final concentration of $10^{-6}$ M and then electrosprayed at a flow rate of about 1 µL min$^{-1}$. The N-terminal of the peptide FAP was acetylated at room temperature for 2 h (pyridine/acetic anhydride; 30:70, v/v) before cleavage from the solid phase.

**Ab initio calculations**: All calculations were performed using the Gaussian 03 series of programs.[35] The geometries of the model species relevant to the suggested EDD mechanism were optimized at the DFT (density functional theory) B3LYP level of theory using the 6-31+G(d,p) basis set. For higher accuracy, single-point energies of optimized structures were calculated at the same level of theory using the 6-311+G(2 d,2p) basis set after adding both polarization and diffuse functions for heavy atoms and hydrogens. The use of diffuse functions is required for structure optimization of electron-rich radical and anionic molecules.[36] Transition-state (TS) structures were identified and optimized by the QST3

method, starting from the optimized minimum-energy structures on both sides of the first-order saddle point and a guess (optimized by a semiempirical method) of the TS structure. The harmonic vibrational frequencies of different stationary points on the potential energy surface (PES) were calculated at the same level of theory as used for their optimization in order to identify local minima or TS. Zero-point energies (ZPE) were computed and adjusted by an appropriate correction factor of 0.9613 for the B3LYP level of theory.[37] The zero-point-corrected energies were then combined with the total energies resulting from the geometry optimizations.

## Acknowledgements

[1] a) A. Pandey, M. Mann, *Nature* **2000**, *405*, 837–846; b) I. Rajagopal, K. Ahern, *Science* **2001**, *294*, 2571–2573.

[2] a) N. L. Kelleher, H. Y. Lin, G. A. Valaskovic, D. J. Aaserud, E. K. Fridriksson, F. W. McLafferty, *J. Am. Chem. Soc.* **1999**, *121*, 806–812; b) F. W. McLafferty, E. K. Fridriksson, D. M. Horn, M. A. Lewis, R. A. Zubarev, *Science* **1999**, *284*, 1289–1290; c) F. Y. Meng, B. J. Cargile, L. M. Miller, A. J. Forbes, J. R. Johnson, N. L. Kelleher, *Nat. Biotechnol.* **2001**, *19*, 952–957; d) S. K. Sze, Y. Ge, H. B. Oh, F. W. McLafferty, *Anal. Chem.* **2003**, *75*, 1599–1603.

[3] a) T. S. Jardetzky, W. S. Lane, R. A. Robinson, D. R. Madden, D. C. Wiley, *Nature* **1991**, *353*, 326–329; b) R. Aebersold, M. Mann, *Nature* **2003**, *422*, 198–207; c) M. S. Boguski, M. W. McIntosh, *Nature* **2003**, *422*, 233–237.

[4] D. F. Hunt, J. R. Yates, J. Shabanowitz, S. Winston, C. R. Hauer, *Proc. Natl. Acad. Sci. USA* **1986**, *83*, 6233–6237.

[5] a) P. Roepstorff, J. Fohlman, *Biomed. Mass Spectrom.* **1984**, *11*, 601; b) K. Biemann, *Biomed. Environ. Mass Spectrom.* **1988**, *16*, 99–111.

[6] F. Kjeldsen, K. F. Haselmann, B. A. Budnik, F. Jensen, R. A. Zubarev, *Chem. Phys. Lett.* **2002**, *356*, 201–206.

[7] R. A. Zubarev, N. L. Kelleher, F. W. McLafferty, *J. Am. Chem. Soc.* **1998**, *120*, 3265–3266.

[8] a) E. Mirgorodskaya, P. Roepstorff, R. A. Zubarev, *Anal. Chem.* **1999**, *71*, 4431–4436; b) K. Hakansson, H. J. Cooper, M. R. Emmett, C. E. Costello, A. G. Marshall, C. L. Nilsson, *Anal. Chem.* **2001**, *73*, 4530–4536; c) A. Stensballe, O. N. Jensen, J. V. Olsen, K. F. Haselmann, R. A. Zubarev, *Rapid Commun. Mass Spectrom.* **2000**, *14*, 1793–1800; d) R. L. Kelleher, R. A. Zubarev, K. Bush, B. Furie, B. C. Furie, F. W. McLafferty, C. T. Walsh, *Anal. Chem.* **1999**, *71*, 4250–4253.

[9] a) K. F. Haselmann, B. A. Budnik, J. V. Olsen, M. L. Nielsen, C. A. Reis, H. Clausen, A. H. Johnsen, R. A. Zubarev, *Anal. Chem.* **2001**, *73*, 2998–3005; b) S. D. H. Shi, M. E. Hemling, S. A. Carr, D. M. Horn, I. Lindh, F. W. McLafferty, *Anal. Chem.* **2001**, *73*, 19–22; c) H. Niiranen, B. A. Budnik, R. A. Zubarev, S. Auriola, S. Lapinjoki, *J. Chromatogr. A* **2002**, *962*, 95–103.

[10] K. F. Haselmann, T. J. D. Jorgensen, B. A. Budnik, F. Jensen, R. A. Zubarev, *Rapid Commun. Mass Spectrom.* **2002**, *16*, 2260–2265.

[11] F. Kjeldsen, K. F. Haselmann, E. S. Sorensen, R. A. Zubarev, *Anal. Chem.* **2003**, *75*, 1267–1274.

[12] F. Kjeldsen, R. Zubarev, *J. Am. Chem. Soc.* **2003**, *125*, 6628–6629.

[13] J. Wong, S. B. Hutchings, R. K. H. Liem, *J. Biol. Chem.* **1984**, *259*, 10867–10874.

[14] P. A. Baeuerle, W. B. Huttner, *J. Biol. Chem.* **1985**, *260*, 6434–6439.

[15] S. Quiroga, K. H. Pfenninger, *J. Neurochem.* **1994**, *63*, 1150–1158.

[16] R. A. Edwards, H. Herrerasosa, J. Otto, J. Bryan, *J. Biol. Chem.* **1995**, *270*, 10764–10770.

[17] a) S. T. Steinborner, J. H. Bowie, *Rapid Commun. Mass Spectrom.* **1996**, *10*, 1243–1247; b) S. T. Steinborner, J. H. Bowie, *Rapid Commun. Mass Spectrom.* **1997**, *11*, 253–258; c) R. A. J. O'Hair, S. Blanksby, M. Styles, J. H. Bowie, *Int. J. Mass Spectrom.* **1999**, *183*, 203–211; d) C. S. Brinkworth, S. Dua, A. M. McAnoy, J. H. Bowie, *Rapid Commun. Mass Spectrom.* **2001**, *15*, 1965–1973; e) G. A. Chass, C. N. J. Marai, A. G. Harrison, I. G. Csizmadia, *J. Phys. Chem. A* **2002**, *106*, 9695–9704.

[18] J. H. Bowie, C. S. Brinkworth, S. Dua, *Mass Spectrom. Rev.* **2002**, *21*, 87–107.

[19] a) N. P. Ewing, C. J. Cassady, *J. Am. Soc. Mass Spectrom.* **2001**, *12*, 105–116; b) P. Boontheung, P. F. Alewood, C. S. Brinkworth, J. H. Bowie, P. A. Wabnitz, M. J. Tyler, *Rapid Commun. Mass Spectrom.* **2002**, *16*, 281–286.

[20] B. A. Budnik, K. F. Haselmann, R. A. Zubarev, *Chem. Phys. Lett.* **2001**, *342*, 299–302.

[21] K. F. Haselmann, B. A. Budnik, F. Kjeldsen, M. L. Nielsen, J. V. Olsen, R. A. Zubarev, *Eur. J. Mass Spectrom.* **2002**, *8*, 117–121.

[22] Y. Ge, B. G. Lawhorn, M. El Naggar, E. Strauss, J. H. Park, T. P. Begley, F. W. McLafferty, *J. Am. Chem. Soc.* **2002**, *124*, 672–678.

[23] F. Kjeldsen, K. F. Haselmann, B. A. Budnik, E. S. Sorensen, R. A. Zubarev, *Anal. Chem.* **2003**, *75*, 2355–2361.

[24] M. S. Thompson, W. Cui, J. P. Reilly, in *ASMS*, ASMS, TN, USA, **2004**.

[25] M. S. Thompson, W. Cui, J. P. Reilly, in *ASMS*, TN, USA, **2004**.

[26] N. L. Clipston, J. Jai-nhuknan, C. J. Cassady, *Int. J. Mass Spectrom.* **2003**, *222*, 363–381.

[27] D. Bilusich, C. S. Brinkworth, J. H. Bowie, *Rapid Commun. Mass Spectrom.* **2004**, *18*, 544–552.

[28] D. F. Liu, T. Wyttenbach, C. J. Carpenter, M. T. Bowers, *J. Am. Chem. Soc.* **2004**, *126*, 3261–3270.

[29] B. A. Budnik, M. L. Nielsen, J. V. Olsen, K. F. Haselmann, P. Horth, W. Haehnel, R. A. Zubarev, *Int. J. Mass Spectrom.* **2002**, *219*, 283–294.

[30] J. E. Bartmess, *Negative Ion Energetics Data*, National Institute of Standards and Technology, Gaithersburg, MD 20899 (http://webbook.nist.gov). **2003**.

[31] a) H. Oh, K. Breuker, S. K. Sze, Y. Ge, B. K. Carpenter, F. W. McLafferty, *Proc. Natl. Acad. Sci. USA* **2002**, *99*, 15863–15868; b) K. Breuker, H. B. Oh, D. M. Horn, B. A. Cerda, F. W. McLafferty, *J. Am. Chem. Soc.* **2002**, *124*, 6407–6420.

[32] M. Mann, O. N. Jensen, *Nat. Biotechnol.* **2003**, *21*, 255–261.

[33] I. A. Ivonin, R. A. Zubarev, in *51st ASMS Conference*, ASMS, Montreal, Canada, **2003**.

[34] L. A. Carpino, G. Y. Hann, *J. Org. Chem.* **1972**, *37*, 3404–3409.

[35] M. J. Frisch et al., Revision B.05 ed., Pittsburgh, PA, **2003**.

[36] a) R. Q. Zhang, J. H. Huang, Y. X. Bu, K. Han, S. T. Lee, G. Z. He, *Science in China Series B-Chemistry* **2000**, *43*, 375–388; b) O. Dolgounitcheva, V. G. Zakrzewski, J. V. Ortiz, *Chem. Phys. Lett.* **1999**, *307*, 220–226.

[37] M. W. Wong, *Chem. Phys. Lett.* **1996**, *256*, 391–399.